

Axial compression tests of RC columns confined by aramid fiber belt prestressing

K. Nakada & T. Yamakawa
University of the Ryukyus, Okinawa, Japan

ABSTRACT: The seismic retrofit technique of aramid fiber belt with initial prestressing was proposed by Yamakawa et al. in 2001, and it was verified that the seismic performance of poor RC columns could be improved by the proposed method. However, the axial compression behavior of RC columns confined by the proposed method has yet to be investigated. In this paper, axial compression tests of RC columns confined by this technique with active and passive confinement were conducted, and the axial compression behavior was investigated thoroughly.

1 INTRODUCTION

The lessons learnt by recent large scale earthquakes, such as the 1995 Hyogoken-Nanbu Earthquake in Japan have reminded that the seismic retrofit must be promoted to existing RC buildings and bridges designed with inadequate old seismic design codes so as to meet the requirements of current seismic design standards. RC buildings built with inadequate old seismic design codes have many columns with poor hoop ratio, and thus earthquake causes brittle shear failure of these columns. Considering this fact, as a dry process, a seismic or emergency retrofit concept of RC column using a new FRP material as aramid fiber belt with initial prestressing was proposed by T. Yamakawa (Yamakawa et al. 2001).

An important aspect of this technique is that the initial prestressing can be introduced into column through aramid fiber belts with the help of coupler. Thus, the benefits of active and passive confinement as well as shear reinforcement can be captured. Therefore, this method is expected to be used for shear critical sound RC columns as a seismic retrofit technique as well as for shear damaged RC columns as an emergency retrofit technique, which is indispensable for the rehabilitation of damaged RC buildings immediately after earthquake attack. The recent investigations have revealed that the failure mode of RC columns with poor hoop arrangement retrofitted by aramid fiber belt prestressing could be changed from brittle shear to flexural one with high ductility (Yamakawa et al. 2001). In addition, by applying this emergency retrofit technique on damaged RC columns, the recovery of seismic performance at various damage levels were also confirmed (Kinjo et al. 2005). Three points worth noting of compressive behavior of RC column externally confined by aramid fiber belt prestressing are as follows:

1. The proposed method can ensure active and passive confinement, and this remarkable idea can derive maximum performance from high strength aramid fiber belt.
2. When the RC column confined by ordinary transverse reinforcement reaches to compressive strength, the hoops in RC column yield at the peak point of stress-strain curve. On the other hand, it is verified that under continuous axial load, the confining pressure by aramid fiber belts in column after reaching to its compressive strength increases linearly due to elastic property of aramid fiber belts.
3. Beyond the compressive strength under the volumetric dilatation, aramid fiber belt works as elastic tensile material because of its fiber material without flexural rigidity.

Therefore, to establish the constitutive law of confined concrete, axial compression tests of RC columns externally confined by aramid fiber belt prestressing were conducted. From the ex-

perimental observations, the stress-strain relationships of concrete and aramid fiber belts are thoroughly investigated in this paper.

2 TEST PLAN

2.1 Axial compression specimens

The retrofit details of typical axial compression specimens are shown in Figure 1a, b, and the cross section is shown in Figure 1c. The column specimens used in this experiment are square column with cross sectional dimension of 250x250mm and height of 750mm. Two types of specimens are considered. One is pure concrete column without steel reinforcement to investigate the lateral confinement effect of aramid fiber belts. The other is RC columns with poor arrangement of transverse reinforcement ($p_w=0.08\%$, $3.7\phi\text{-}@105$). Hoops are arranged closely at top and bottom ends of each specimen within the length of 125mm like a stub to ensure damage at the central height of column (see Fig. 1a and b). Aramid fiber belt is cut and impregnated with epoxy resin along only 100mm lap joint to form a loop of two-ply belt. The two-ply belt is wound around the column through corner angles located at the corners of column and clamped together at both ends of the two-ply belt by a couple of cross-bars, namely coupler, which is screwed manually to apply the pretension into belts (see Fig. 1c). To control and measure the tension strain, strain gauges are attached to the belt surface which is locally impregnated with epoxy resin. Two types of aramid fiber belts are used in this experiment, namely single-type belt with width of 17mm and double-type belt with width two times that of single-type. The mechanical properties of aramid fiber belts, steel materials and concrete are shown in Table 1, Table 2 and Table 3 respectively. To avoid the bleeding effect, horizontal casting of concrete was done in all specimens. The experimental parameters are longitudinal reinforcement ratio(0.45, 0.9, 1.36%), interval of aramid fiber belt(65, 95, 130mm), type of belt(single, double) and initial tension strain level(0.1, 0.2, 0.35, 0.52, 0.7%). Non-retrofitted specimens are considered to compare with axial compression behavior of retrofitted ones. The details of specimens and experimental parameters are shown in Table 3. The total number of specimens is 45.

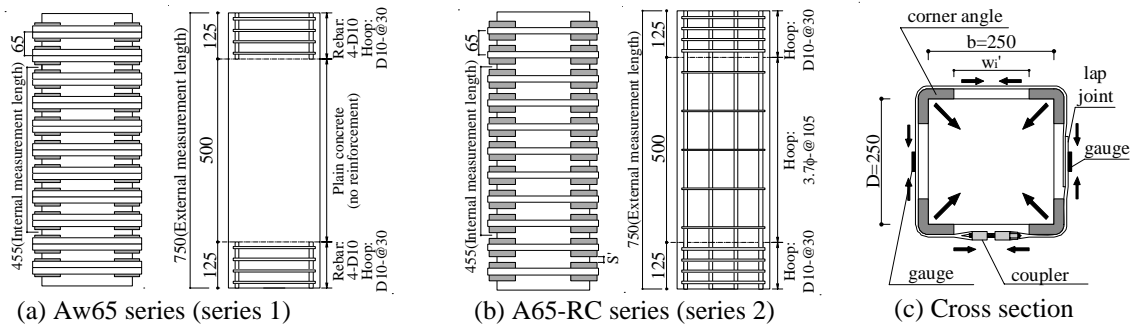


Figure 1. Uniaxial compression specimens.

Table 1. Mechanical properties of aramid fiber belt.

Aramid fiber belt	Cross section (mm ²)	Width (mm)	Thickness (mm)	A (mm ²)	Aw (mm ²)	σ_u (MPa)	ε_u (%)	A_E (GPa)
	9.72	17	0.572	19.44	38.88	2380	2.22	107

*A= single belt, Aw= double belt, σ_u =ultimate strength of aramid fiber belts, ε_u =ultimate strain of aramid fiber belts, A_E =Young's modulus of elasticity.

Table 2. Mechanical properties of steel reinforcement.

Steel reinforcement	A (mm ²)	E (GPa)	σ_y (MPa)	σ_u (MPa)
Rebar	D10	71	202	349
Hoop	3.7 ϕ	11	208	650

*A= cross sectional area, E= Young's modulus of elasticity, σ_y = yield strength of steel, σ_u = ultimate strength of steel.

Table 3. Details of test specimens and test results.

Series	Specimen	ϵ_{pt}	A^S	$c\sigma_B$	$c\sigma_{cB}$	
		%	mm	MPa	MPa	
1	AC07M-1	-	-	26	20.8	
	AC07M-2	-	-		17.2	
	AC07M-3	-	-		18.4	
	AC07M-Aw65H	0.70	65		26.5	
	AC07M-Aw65H	0.70	65		25.4	
	AC07M-Aw95H	0.70	95		23.9	
	AC07M-A65ML	0.10	65		20.0	
	AC07M-A65MM	0.20	65		20.6	
	AC06M-1	-	-		33	26.7
	AC06M-2	-	-			25.9
	AC06M-Aw130N	0	130	27.7		
	AC06M-Aw130M	0.35	130	28.3		
	AC06M-Aw130H	0.70	130	30.4		
	AC06M-3	-	-	30	23.4	
	AC06M-4	-	-		22.9	
	AC06M-Aw65N	0	65		24.3	
	AC06M-Aw65M	0.35	65		27.0	
	AC06M-Aw65MH	0.52	65		28.9	
	AC06M-Aw65H	0.70	65		30.9	
	AC05M-1	-	-		23	19.4
	AC05M-2	-	-	19.9		
	AC05M-A65N	0	65	20.6		
	AC05M-A65M	0.35	65	22.5		
	AC05M-A65H	0.70	65	24.9		
	AC05M-A130N	0	130	20.3		
	AC05M-A130M	0.35	130	21.7		
AC05M-A130H	0.70	130	22.7			
2	AC07M-4	-	-	32		22.2
	AC07M-5	-	-		23.1	
	AC07M-A65MR8	0.91	0.35		65	22.6
	AC07M-A65MR8	0.91	0.35		65	23.9
	AC07M-A65MR12	1.36	0.35		65	23.0
	AC06M-RC12-5	1.36	-	33	23.9	
	AC06M-RC12-6	1.36	-		23.8	
	AC06M-RC4-7	0.45	-		23.9	
	AC06M-RC12-8	1.36	-	30	22.4	
	AC06M-RC8-9	0.91	-		23.2	
	AC06M-RC4-10	0.45	-		22.5	
	AC06M-A65NR12	1.36	0	65	33	23.1
	AC06M-A65MR12	1.36	0.35	65	30	25.0
	AC06M-A65MR8	0.91	0.35	65	30	24.6
AC06M-A65HR8	0.91	0.70	65	30	26.5	
AC06M-A65NR4	0.45	0	65	33	24.2	
AC06M-A65MR4	0.45	0.35	65	30	24.9	
AC06M-A65HR4	0.45	0.70	65	33	27.7	

*Aw: double belt, A: single belt, 65: interval of aramid fiber belt, N: initial strain level of aramid fiber belt (N: 0%, ML: 0.1%, MM: 0.2%, M: 0.35%, MH: 0.52%, H: 0.7%)
R12: number of rebar (12)

** p_g = longitudinal reinf. ratio, ϵ_{pt} = initial tensile strain, A^S = interval of aramid fiber belts, $c\sigma_B$ =cylinder strength of concrete, $c\sigma_{cB}$ =compressive strength of confined concrete.

2.2 Test apparatus and measurement setup

Test apparatus (Universal testing machine) and measurement setup for axial compression specimens are illustrated in Figure 2. The capacity of test apparatus is 2000kN. The axial compression load is applied to specimens monotonically under the condition of top end with free rotation and fixed bottom end. To measure the axial strain, eight transducers were arranged between two loading plates and at the central part of the column as shown in Figure 2. To describe the experimental stress-strain curves, the measured axial strain by four transducers located at the central part of the column is adopted until the peak point of stress-strain curve, and the measured axial strain between two loading plates is only used for the descending portion of the stress-strain curve.

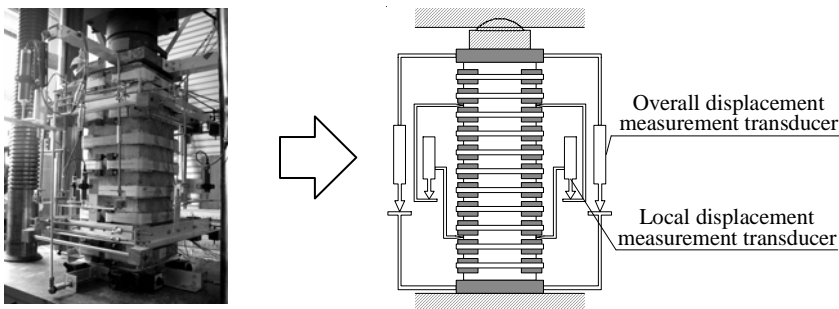


Figure 2. Test apparatus and measurement setup.

3 EXPERIMENTAL RESULTS AND DISCUSSIONS

3.1 Measured stress-strain curves

The experimental stress-strain curves of confined concrete of series 1 are shown in Figure 3, where the vertical axis ($\sigma_c/c\sigma_p$) is defined as the ratio of the compressive stress(σ_c) of retrofitted specimens to the experimental compressive strength of non-retrofitted one ($c\sigma_p$), and the compressive stress is defined as the axial force of concrete divide by the gross sectional area. More-

over, the axial force of steel reinforcements of RC column specimens (series 2) are subtracted from the total axial force. The stress-strain relationship of steel reinforcement used in this calculation was assumed to be the elastic-perfectly plastic approximation. The vertical strain of steel reinforcement was corresponded to the average axial strain of column specimens. In case of non-retrofitted column specimens(series 1), the ratio of the compressive strength of the column specimen to the cylinder strength(σ_p/σ_B) was in the range of 0.74-0.87, while in case of RC column specimens(series 2), the ratio(σ_p/σ_B) was in the range of 0.71- 0.75.

In plain concrete specimens (AC05M-1, AC06M-2, 3), the compressive stress reached to the maximum stress at $\epsilon_c=0.14-0.18$, where ϵ_c is the axial strain. Beyond the compressive strength, the compressive stress decreased sharply as shown in Figure 3.

In specimens A65N, A130N, Aw65N and Aw130N, which were confined by aramid fiber belt without initial prestressing, namely non-prestressed specimens, the compressive strength was almost the same as that of the non-retrofitted specimens. Beyond the compressive strength, the axial stress of these column specimens sharply decreased to a certain axial strain, which indicated that the large confinement effect of aramid fiber belts began to appear, and the descending branch of the experimental stress-strain curve dropped less quickly or increased gradually due to the large confining pressure of aramid fiber belt. On the other hand, in column specimens confined by aramid fiber belts with initial prestressing, it was observed that the compressive strength increased as the initial tension strain level increased and beyond the compressive strength, the axial stress decreased more gradually compared to the non-prestressed specimens. In case of prestressed specimens, it was observed that the effect of volumetric ratio of aramid fiber belt to descending branch was larger than that of the initial strain level.

In case of non-prestressed specimens, the existence of looseness of aramid fiber belt caused the steep degradation of the axial stress beyond the peak point of the stress-strain curve. By maintaining the large confining pressure of aramid fiber belts, the sharp degradation of the descending branch can be prevented.

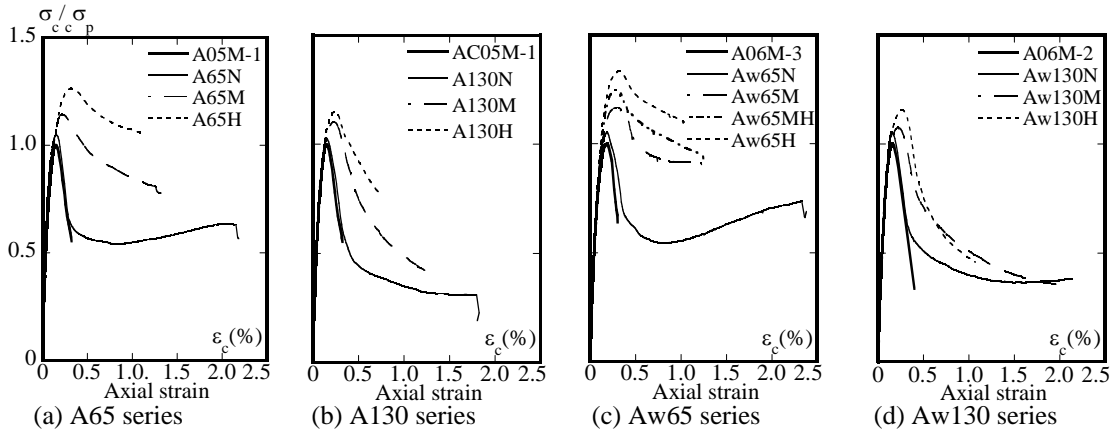


Figure 3. Measured stress-strain curves of confined concrete (series1).

3.2 Strain of aramid fiber belt

The relation between the strain of aramid fiber belt and the compressive strain of confined concrete(series 1) is shown in Figure 4. This Figure shows the typical strain among the aramid fiber belts throughout the column's height. The dotted line (ϵ_0) shows the compressive strain at the peak point of the stress-strain curve of the non-retrofitted specimens, and the black mark shows the peak point of the stress-strain curve of the retrofitted one. In specimen AC07M-Aw65H and AC06M-Aw65H, the initial tensile force introduced in aramid fiber belt through corner angles placed at four corners of column causes bearing stress of about 12.5MPa.

In Figure 4, it is observed that the strain of aramid fiber belt of non-prestressed column specimens is extremely low until black marks (on an average of 120μ at peak point of the stress-strain curve) and after that the strain increases progressively. This also indicates that the passive confinement increases gradually beyond the compressive strength due to the elastic property of aramid fiber belts. Therefore, by using aramid fiber belts, this lateral confinement can considerably improved the descending portion of the stress-strain curve of the non-prestressed one. On

the other hand, in prestressed specimens, the behavior of aramid fiber belt strains is almost the same as non-prestressed one, but the increment of aramid fiber belt strain from initial strain level at peak point of the stress-strain curve is larger than that of the non-prestressed one (on an average of 570μ).

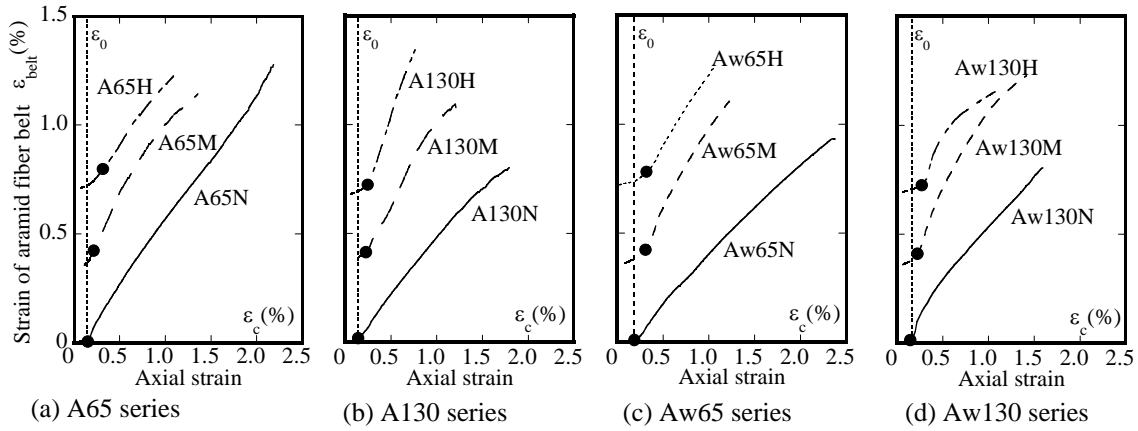


Figure 4. Strain of aramid fiber belt versus axial strain of confined concrete (series1).

3.3 Strength enhancement of confined concrete

As discussed in section 3.1, by applying initial prestressing through aramid fiber belts, the compressive strength of confined concrete can be enhanced. The strength enhancement of confined concrete is assessed quantitatively in this section. Here, the strength enhancement ratio is defined as the experimental compressive strength of retrofitted specimens divided by that of non-retrofitted specimens ($K_{exp} = \sigma_{cB} / \sigma_p$).

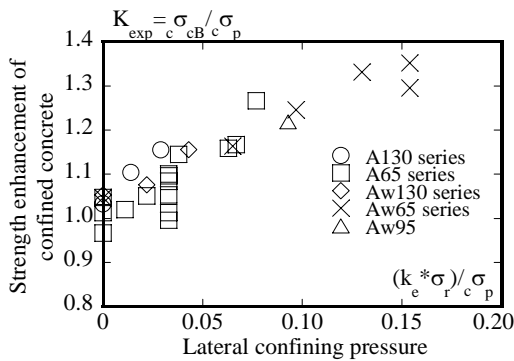
Figure 5 shows the relation between the experimental strength enhancement ratio (K_{exp}) and the lateral confining pressure ($k_e * \sigma_r / \sigma_p$). The lateral confining pressure (σ_r) is expressed as

$$\sigma_r = 0.5 \cdot \rho_A \cdot E_A \cdot \varepsilon_{pt} \quad (1)$$

where ρ_A is volumetric ratio of aramid fiber belt, E_A is Young's modulus of aramid fiber belt, and ε_{pt} is the initial strain level of aramid fiber belt. Here, the confinement effectiveness coefficient (k_e), which is based on Mander's concept (Mander et al. 1988), is taken into account to calculate the lateral confining pressure. The effectively confined area is clearly observed after the end of axial compression test as shown in Figure 5b. This is expressed as

$$k_e = \left\{ 1 - \sum_{i=1}^n \frac{(w_i')^2}{6 \cdot b^2} \right\} \left(1 - \frac{s'}{2 \cdot b} \right)^2 \quad (2)$$

where w_i' is the clear distance between corner angles placed in column (see Fig. 1), s' is the clear distance between the adjacent corner angles in vertical direction, n is the number of corner



(a) Strength enhancement ratio

(b) Observed effective confining area

Figure 5. Experimental strength enhancement ratio of confined concrete.

angles. A good correlation between K_{exp} and $k_e \cdot \sigma_r / \sigma_p$ (correlation coefficient is 0.92) is observed in Figure 5. It is important to note that in case of large lateral confining pressure, K_{exp} seems to reach the peak of $K_{exp} - k_e \cdot \sigma_r / \sigma_p$ relationship. It is understood that the peak of strength enhancement ratio indicates the limitation of active confinement effect.

3.4 Compressive strain at peak point of confined concrete

The relationship of experimental compressive strain of confined concrete (ϵ_{cB}) and the strength enhancement ratio (K_{exp}) is shown in Figure 6. Here, it is observed that as the strength enhancement ratio (K_{exp}) increases, the compressive strain (ϵ_{cB}) increases. It is also observed that in case of column specimens with steel reinforcement, the steel reinforcement ratio does not affect the compressive strain as shown by black marks in Figure 6.

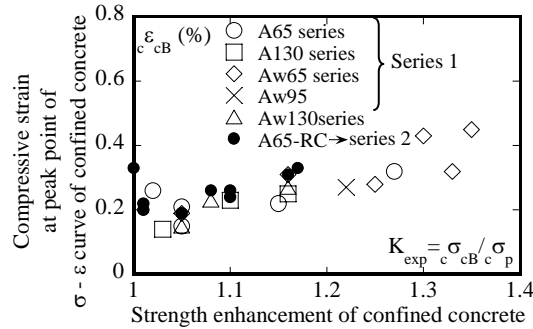


Figure 6. Compressive strain at peak point of stress-strain curve of confined concrete.

4 CONCLUSIONS

- 1) The lateral confinement technique using aramid fiber belt with initial prestressing enhances the compressive strength of the confined concrete.
- 2) In prestressed column specimens, the volumetric ratio of aramid fiber belt affects the descending branch of the stress-strain curve.
- 3) The experimental strength enhancement ratio of the confined concrete reaches to the upper limit. This indicates the limitation of the active confinement effect.
- 4) The correlation between the compressive strain of the confined concrete and the strength enhancement ratio was confirmed.

In this paper, the axial compression behavior of RC columns confined by aramid fiber belt prestressing was investigated through the axial compression test. Therefore, considering these facts, the constitutive law of confined concrete will be established in the near future.

ACKNOWLEDGMENTS

The investigation was supported by the Grant-in-Aid for Young Scientists (B), (18760423), 2006-2007, by the ministry of Education, Culture, Sports, Science and Technology. The authors wish to acknowledge Dr. Md. Nafiur Rahman, postdoctoral researcher and Mr. Pasha Javadi, doctoral student, Dept. of Civil Eng. and Arch., Univ. of the Ryukyus for their valuable advice.

REFERENCES

- Mander, J. B., Priestley, M. J. N. and Park, R. (1988). Theoretical Stress-Strain Model for Confined Concrete. *Journal of Structural Engineering, ASCE*, 114(8), 1804- 1826.
- Yamakawa, T., Nesheli, K. N., Satoh, H. (2001). Seismic or Emergency Retrofit of RC Short Columns by Use of Prestressed Aramid Fiber Belts as External Hoops. *J. Struc. Constr. Eng., AIJ*, 550, 135- 141.
- Kinjo, H., Yamakawa, T., Fujikawa, S. and Nakada, K. (2005). Emergency Retrofit for shear Damaged Short RC Columns Utilizing Pre-tensioned Aramid Fiber Belts. *Proc. of the Japan Concrete Institute(JCI)*, 27(1), 1447- 1452. (in Japanese)